Doppler imaging of plasma modes in a Penning trap[†]

**T. B. Mitchell, J. J. Bollinger, X.-P. Huang,
and W. M. Itano**

*Time and Frequency Division, National Institute of Standards and Technology,
Boulder, CO 80303*

travis.mitchell@nist.gov

Abstract: We describe a technique and present results for imaging the modes of a laser-cooled plasma of $^9Be^+$ ions in a Penning trap. The modes are excited by sinusoidally time-varying potentials applied to the trap electrodes. They are imaged by changes in the ion resonance fluorescence produced by Doppler shifts from the coherent ion velocities of the mode. For the geometry and conditions of this experiment, the mode frequencies and eigenfunctions have been calculated analytically. A comparison between theory and experiment for some of the azimuthally symmetric modes shows good agreement.

[†] *Work of the U.S. Government. Not subject to U.S. copyright.*

References

1. *Non-Neutral Plasma Physics II*, eds. J. Fajans and D. H. E. Dubin (AIP, New York, 1995).

2. J. H. Malmberg and T. M. O'Neil, "Pure electron plasma, liquid, and crystal," *Phys. Rev. Lett.* **39**, 1333-1336 (1977).

3. C. F. Driscoll, J. H. Malmberg, and K. S. Fine, "Observation of transport to thermal equilibrium in pure electron plasmas," *Phys. Rev. Lett.* **60**, 1290-1293 (1988).

4. L. R. Brewer, J. D. Prestage, J. J. Bollinger, W. M. Itano, D. J. Larson, and D. J. Wineland, "Static properties of a non-neutral $^9Be^+$ ion plasma," *Phys. Rev. A* **38**, 859-873 (1988).

5. J. J. Bollinger, D. J. Wineland, and D. H. E. Dubin, "Non-neutral ion plasmas and crystals, laser cooling, and atomic clocks," *Phys. Plasmas* **1**, 1403-1414 (1994).

6. D. H. E. Dubin, "Theory of electrostatic fluid modes in a cold spheroidal non-neutral plasma," *Phys. Rev. Lett.* **66**, 2076-2079 (1991).

7. J. J. Bollinger, D. J. Heinzen, F. L. Moore, W. M. Itano, D. J. Wineland, and D. H. E. Dubin, "Electrostatic modes of ion-trap plasmas," *Phys. Rev. A* **48**, 525-545 (1993).

8. R. G. Greaves and C. M. Surko, "Antimatter plasmas and antihydrogen," *Phys. Plasmas* **4**, 1528-1543 (1997).

9. G. Gabrielse, X. Fei, L. A. Orozco, R. L. Tjoelker, J. Haas, H. Kalinowsky, T. A. Trainor, and W. Kells, "Cooling and slowing of trapped antiprotons below 100 meV," *Phys. Rev. Lett.* **63,** 1360 (1989).

10. M. H. Holzscheiter, X. Feng, T. Goldman, N. S. P. King, R. A. Lewis, M. M. Nieto, and G. A. Smith, "Are antiprotons forever?," *Phys. Lett. A* **214,** 279 (1996).

11. D. J. Heinzen, J. J. Bollinger, F. L. Moore, W. M. Itano, and D. J. Wineland, "Rotational equilibria and low-order modes of a non-neutral ion plasma," *Phys. Rev. Lett.* **66**, 2080-2083 (1991).

12. X.-P. Huang, J. J. Bollinger, T. B. Mitchell, and W. M. Itano, "Phase-locked rotation of crystallized non-neutral plasmas by rotating electric fields," *Phys. Rev. Lett.* **80**, 73-76 (1998).

13. D. H. E. Dubin and J. P. Schiffer, "Normal modes of cold confined one-component plasmas," *Phys. Rev. E* **53**, 5249-5267 (1996).

14. D. H. E. Dubin, "Effects of correlations on the thermal equilibrium and normal modes of a non-neutral plasma," *Phys. Rev. E* **53**, 5268-5290 (1996).

15. C. S. Weimer, J. J. Bollinger, F. L. Moore, and D. J. Wineland, "Electrostatic modes as a diagnostic in Penning trap experiments," *Phys. Rev. A* **49**, 3842-3853 (1994).

16. M. D. Tinkle, R. G. Greaves, and C. M. Surko, "Low-order longitudinal modes of single-component plasmas," *Phys. Plasmas* **2**, 2880-2894 (1995).

17. R. G. Greaves, M. D. Tinkle, and C. M. Surko, "Modes of a pure ion plasma at the Brillouin limit," *Phys. Rev. Lett.* **74**, 90-93 (1995).

18. C. F. Driscoll, "Observation of an unstable $m = 1$ diocotron mode on a hollow electron column," *Phys. Rev. Lett.* **64**, 1528-1543 (1990).

19. J. N. Tan, J. J. Bollinger, B. Jelenković, and D. J. Wineland, "Long-range order in laser-cooled, atomic-ion Wigner crystals observed by Bragg scattering," *Phys. Rev. Lett.* **75**, 4198-4201 (1995).

20. W. M. Itano, J. J. Bollinger, J. N. Tan, B. Jelenković, X.-P. Huang, and D. J. Wineland, "Bragg diffraction from crystallized ion plasmas," *Science* **279**, 686-689 (1998).

21. Here ω_{lm} is the mode frequency in a frame rotating with the plasma. For the $m = 0$ modes discussed here this distinction is not necessary because their frequency is the same in either the laboratory or rotating frame.

22. Information on the mode eigenfunction can be obtained from the side-view images even when there is a change in the phase-averaged ion fluorescence. However, the images may no longer provide a linear measure of the mode axial velocity.

23. R. C. Thompson, K. Dholakia, J-L. Hernandez-Pozos, G. Zs. K. Horvath, J. Rink, and D. M. Segal, "Spectroscopy and quantum optics with ion traps," *Phys. Scr.* **T72**, 24-33 (1997).

1. Introduction

Non-neutral plasmas consisting exclusively of particles of a single sign of charge have been used to study many basic processes in plasma physics [1], partly because non-neutral (as opposed to neutral or quasi-neutral) plasmas can be confined by static electric and magnetic fields and also be in a state of global thermal equilibrium [2–4]. A particularly simple confinement geometry for non-neutral plasmas is the quadratic Penning trap, which uses a strong uniform magnetic field $\mathbf{B_0} = B_0\hat{\mathbf{z}}$ superimposed on a quadratic electrostatic potential

$$\phi_T(r,z) = \frac{m\omega_z^2}{2q}\left(z^2 - \frac{r^2}{2}\right). \tag{1}$$

Here m and q are the mass and charge of a trapped ion, and ω_z is the axial frequency of a single ion in the trap. The global thermal equilibrium state for a single charged species in a quadratic Penning trap has been well studied [4,5]. For sufficiently low temperatures, the plasma takes on the simple shape of a uniform density spheroid. An interesting result is that all of the electrostatic modes of a magnetized, uniform density spheroidal plasma can be calculated analytically [6,7]. This is the only finite length geometry for which exact plasma mode frequencies and eigenfunctions have been calculated for a realistic thermal equilibrium state. In this manuscript we describe a technique for measuring these frequencies and eigenfunctions, and compare theory predictions and experimental results for some of the azimuthally symmetric modes.

The modes have several potential applications in Penning trap experiments. In general, the mode frequencies depend on the density and shape of the plasma spheroid. Therefore measurement of a mode frequency provides a non-destructive method for obtaining basic diagnostic information about the plasma. This is especially important in anti-matter plasmas [8–10], where conventional techniques for obtaining information about these plasmas involve ejecting the plasma from the trap. Other applications arise from the fact that the modes can strongly influence the dynamical behavior of trapped

plasmas. For example, certain azimuthally asymmetric modes can have zero frequency in the laboratory frame and be excited by a static field error of the trap. These zero frequency modes can strongly limit the achievable density in a Penning trap [11]. Similarly, the plasma angular momentum can be changed through the deliberate excitation of azimuthally asymmetric modes, and the applied torque can be much greater than that from the "rotating wall" perturbation [12], which is not mode-resonant. Finally, the modes may provide useful information on the internal state of a plasma. For example, measurement of the damping of the modes can provide information on the plasma's viscosity. This measurement could presumably be done in the interesting regime where the plasma is strongly correlated [13,14].

Previous experimental mode studies on spheroidal plasmas have been limited to frequency measurements on a small class of modes. With laser-cooled Be^+ ion plasmas, some quadrupole mode frequencies have been measured and agree well with theory [7,11]. Mode frequencies have also been measured on spheroidal cryogenic electron plasmas [15], 0.025–0.5 eV electron and positron plasmas [16], and room temperature Ar^+ ion plasmas [17]. In these cases qualitative agreement with theory was observed and the modes provided some basic diagnostic information. However, deviations from the model of a constant density spheroid in a quadratic trap limited the comparison with the ideal linear theory. Here, in addition to measuring mode frequencies, we also measure the mode eigenfunctions. The eigenfunctions permit direct identification of the modes. In addition, they contain much more information than the frequencies and therefore may be useful for observing nonlinear effects such as mode couplings. Mode eigenfunctions have been measured for low frequency, z-independent (diocotron) modes on cylindrical electron columns [18]. In that work, the mode measurements were important in identifying two coexisting modes.

2. Experimental apparatus

Figure 1 shows a sketch of the apparatus [19,20] used for the mode measurements. The trap consists of a 127 mm long stack of cylindrical electrodes at room temperature with an inner diameter of 40.6 mm, enclosed in a 10^{-8} Pa vacuum chamber. A uniform magnetic field $B_0 = 4.465$ T is aligned parallel to the trap axis within 0.01°, and results in a $^9Be^+$ cyclotron frequency $\Omega = qB_0/m = 2\pi \times 7.608$ MHz. The magnetic field alignment is accomplished by minimizing the excitation of zero-frequency modes produced by a tilt of the magnetic field with respect to the trap electrode symmetry axis [7,11]. Positive ions are confined in this trap by biasing the central "ring" electrode to a negative voltage $-V_0$ with respect to the endcaps. Because the dimensions of the Be^+ plasmas ($\lesssim 2$ mm) are small compared to the diameter of the trap electrodes, the quadratic potential of Eq. (1) is a good approximation for the trap potential. For the work reported here, $V_0 = 2.00$ kV which results in $\omega_z = 2\pi \times 1.13$ MHz and a single particle magnetron frequency $\omega_m = [\Omega - (\Omega^2 - 2\omega_z^2)^{\frac{1}{2}}]/2 = 2\pi \times 84.9$ kHz.

We create a Be^+ plasma by ionizing neutral Be atoms in a separate trap (not shown) and then transferring the ions to the main trap. For the mode work discussed here, the number of ions was typically 6×10^4. While the total charge in the trap is conserved after loading, the relative abundance of contaminant, heavier-mass ions increases, presumably due to reactions between Be^+ ions and background neutral molecules. Because we analyze our experimental results using an existing theory [6] for the electrostatic modes of a single-species plasma, we took data only with relatively clean clouds ($< 3\%$ impurity ions). The plasmas were cleaned approximately every 30 minutes by transferring the ions to the load trap where, with a shallow 3 V deep well, contaminant ions were driven out of the trap by exciting their axial frequencies. Cleaning therefore results in a decrease in the number of trapped ions. Over a 12–14 hour period, the num-
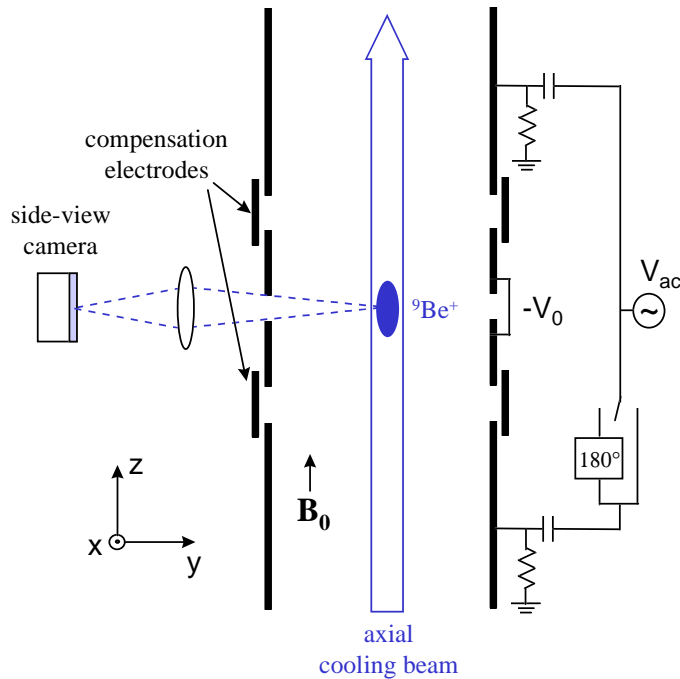
Figure 1. Sketch of the experimental apparatus. Modes were excited by applying in-phase or 180° out-of-phase sinusoidal potentials to the trap endcaps.

ber of ions is reduced by a factor of 2. Because the mode frequencies and eigenfunctions in a quadratic trap are independent of the number of ions, the measurements described here are not affected.

The trapped Be^+ ions are Doppler-cooled by two laser beams at wavelength $\lambda \approx 313.11$ nm. The main cooling beam is directed parallel to $\mathbf{B_0}$ as shown in Fig. 1, and a second beam propagating perpendicular to $\mathbf{B_0}$ (not shown and turned off during the mode eigenfunction measurements) is also used to compress the plasma by applying a radiation pressure torque [4,11]. For mode measurements the axial cooling-laser frequency is fixed about one natural linewidth (~ 20 MHz) below the transition frequency. Ions which, due to excitation of a mode, have an axial velocity $v_z < 0$ therefore fluoresce more strongly than ions with $v_z > 0$. The ion temperature was not measured; however, based on previous work [4], we expect $T \lesssim 20$ mK.

An $f/5$ imaging system detects the Be^+ resonance fluorescence scattered perpendicularly from the axial cooling beam (waist ≈ 0.5 mm, power ≈ 50 μW) to produce a side-view image of the Be^+ ions. The side-view image is obtained with a photon-counting camera system which records the spatial and temporal coordinates of the detected photons. This data is processed to obtain the mode eigenfunctions by constructing side-view images as a function of the phase of the external drive used to excite the modes.

3. Electrostatic modes of a cryogenic plasma

The constant-density, spheroidal plasma model is a good approximation for our work. In thermal equilibrium, a Penning trap plasma rotates as a rigid body at frequency ω_r, where $\omega_m < \omega_r < \Omega - \omega_m$, about the trap's $\hat{\mathbf{z}}$ axis [2,5]. In this work the rotation frequency was precisely set by a rotating dipole electric field [12]. As the ions rotate through the magnetic field they experience a Lorentz force which provides the radial

confining force of the trap. This ω_r-dependent confinement results in an ω_r-dependent ion density and plasma shape. At the low temperatures of this work, the plasma density is uniform over distances large compared to the interparticle spacing ($\sim 10\ \mu$m) and is given by $n_0 = \epsilon_0 m \omega_p^2 / q^2$ where $\omega_p = [2\omega_r(\Omega - \omega_r)]^{\frac{1}{2}}$ is the plasma frequency. With the confining potential of Eq. (1), the plasma is spheroidal with boundary $z^2/z_0^2 + x^2/r_0^2 + y^2/r_0^2 = 1$. The spheroid aspect ratio $\alpha \equiv z_0/r_0$ is determined by ω_r [4,5]. We have neglected the effect of image charges, because the plasma dimensions are small compared to the trap dimensions.

The modes of these spheroidal plasmas can be classified by integers (l, m), where $l \geq 1$ and $0 \leq m \leq l$ [6,7]. For an (l, m) mode with frequency ω_{lm} [21], the perturbed potential of the mode inside the plasma is given by a symmetric product of Legendre functions,

$$\Psi^{lm} \propto P_l^m(\bar{\xi}_1/\bar{d}) P_l^m(\bar{\xi}_2) e^{i(m\phi - \omega_{lm}t)}. \tag{2}$$

Here $\bar{\xi}_1$ and $\bar{\xi}_2$, discussed in Ref. [6], are scaled spheroidal coordinates where the scaling factor depends on the frequencies ω_r, Ω, and ω_{lm}, and $\bar{d}$ is a shape-dependent parameter which also depends on these frequencies. In general, for a given (l, m) there are many different modes. In this paper we report measurements of the mode frequencies and eigenfunctions of a few magnetized plasma modes, which are defined as those modes with frequencies $|\omega_{lm}| < |\Omega - 2\omega_r|$ [6,7]. In addition, we only discuss measurements of azimuthally symmetric ($m = 0$) modes. For $\omega_r \ll \Omega/2$, these modes principally consist of oscillations parallel to the magnetic field at a frequency on the order of ω_z. In the experiment we detect the axial velocity of a mode. In the linear theory, this is proportional to $\partial \Psi^{lm}/\partial z$.

We excite plasma modes by applying sinusoidally time-varying potentials to the trap electrodes. Azimuthally symmetric ($m = 0$) even l modes are excited by applying in-phase potentials to the endcaps (even drive), while odd l modes are excited by applying 180° out-of-phase potentials to the endcaps (odd drive). Azimuthally asymmetric ($m \neq 0$) modes can be excited by applying time-varying potentials to the compensation electrodes, which have 6-fold azimuthal symmetry. In Refs. [7, 11] quadrupole ($l = 2$) mode frequencies were measured by observing the change in the total ion fluorescence from the plasma, averaged over the phase of the drive, which occurred when the drive frequency equaled the mode frequency. However, in order to observe such a change, the mode excitation must be large enough so that either the fluorescence from an ion non-linearly depends on its velocity or there is some heating of the plasma by the mode. The larger amplitude drive required by this technique decreases the precision of the mode measurements.

The new technique reported here entails reducing the drive amplitude until the change in the phase-averaged ion fluorescence is negligible, and detecting the mode's coherent ion velocities by recording side-view images as a function of the phase and frequency of the external drive. These Doppler images provide direct measurements of the mode's axial-velocity eigenfunction [22]. In addition, an accurate measurement of the mode's frequency can be obtained from the line center of the mode amplitude as a function of drive frequency. High order modes have been excited and detected with this technique, such as the $(11, 0)$ and $(12, 1)$ modes. We note that for the $(1, 0)$ and $(1,1)$ modes, imaging is not required because there is no spatial variation in their eigenfunction. The driven mode amplitude and phase of these center-of-mass modes can therefore be obtained by coherently detecting the spatially-integrated fluorescence as a function of the phase of the external drive [23].
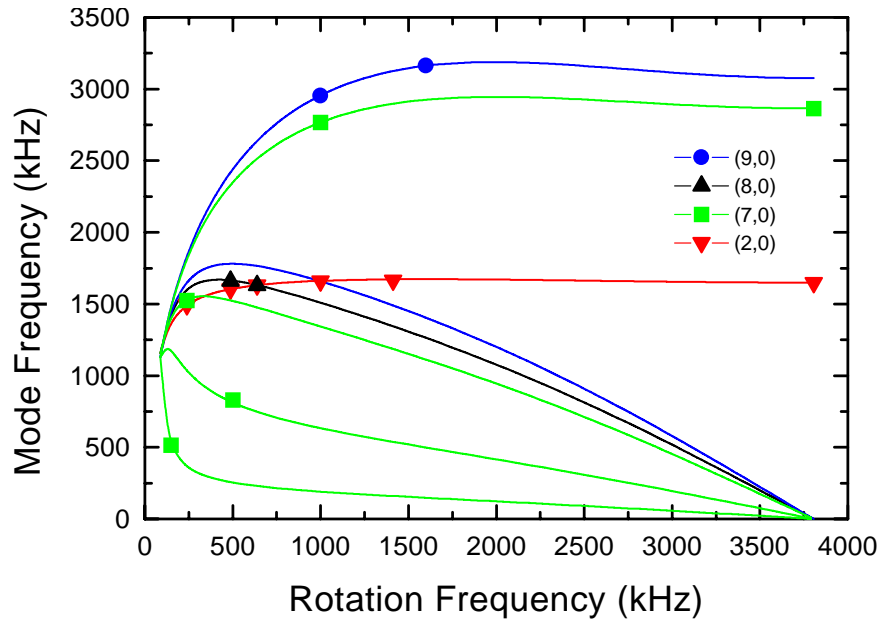
Figure 2.   Plots of the frequencies of several magnetized plasma modes as a function of rotation frequency for $\Omega/2\pi$=7.608 MHz and $\omega_z/2\pi$=1.13 MHz. The solid lines are the theoretical predictions and the symbols are experimental measurements. Only the highest frequency $(9,0)$ plasma mode and the second highest frequency $(8,0)$ plasma mode are plotted.

4.   Experimental results

In Fig. 2 we plot several measured mode frequencies, along with the theoretical predictions, for azimuthally symmetric magnetized plasma modes as a function of ω_r for $\omega_z/2\pi = 1.13$ MHz and $\Omega/2\pi = 7.608$ MHz. Many different mode frequencies at various values of ω_z have been measured, and on clean clouds agreement between the observed and predicted mode frequencies is typically better than 1%. In this manuscript we concentrate on describing the images obtained of the $(2,0)$ and the highest frequency $(9,0)$ magnetized plasma modes. For a given $(l,0)$, the highest frequency magnetized plasma mode does not have any radial nodes.

Figure 3 demonstrates the phase-coherent detection of the $(2,0)$ mode. This is one of the simplest modes that is not merely a center-of-mass oscillation of the plasma. In this mode the plasma stays spheroidal but the aspect ratio (and density) oscillate at $\omega_{2,0}$. For $\omega_r \ll \Omega/2$, the oscillation in r_0 is very small, so the mode principally consists of oscillations in z_0 at $\omega_{2,0}$. Ions above the $z=0$ plane oscillate $180°$ out of phase with ions below $z=0$.

Figure 3(a) shows a sequence of 18 side-view images as a function of the phase of the mode drive at $\omega_{2,0}/2\pi = 1.656$ MHz. The plasma's rotation frequency was set to $\omega_r/2\pi = 1.00$ MHz and the $m = 0$ even drive rms amplitude was 7.07 mV. In the images, the magnetic field and the axial laser beam point up. As expected for the $(2,0)$ mode, the detected fluorescence in the upper half of the plasma is bright when the lower half is dark and vice versa. We analyze the data of Fig. 3(a) by performing a least-squares fit of the intensity at each point to $A_0 + A_{2,0}\cos(\omega_{2,0}t + \varphi_{2,0})$. Figures 3(b) and 3(c) show the resultant images of the measured mode amplitude $A_{2,0}(x,z)$ and phase $\varphi_{2,0}(x,z)$. These are compared with the theoretically predicted values of these quantities. Because the plasma is optically thin, the theoretical predictions were obtained by integrating $\partial\Psi^{lm}/\partial z$ over y. The amplitude of the theoretical prediction is scaled to match the
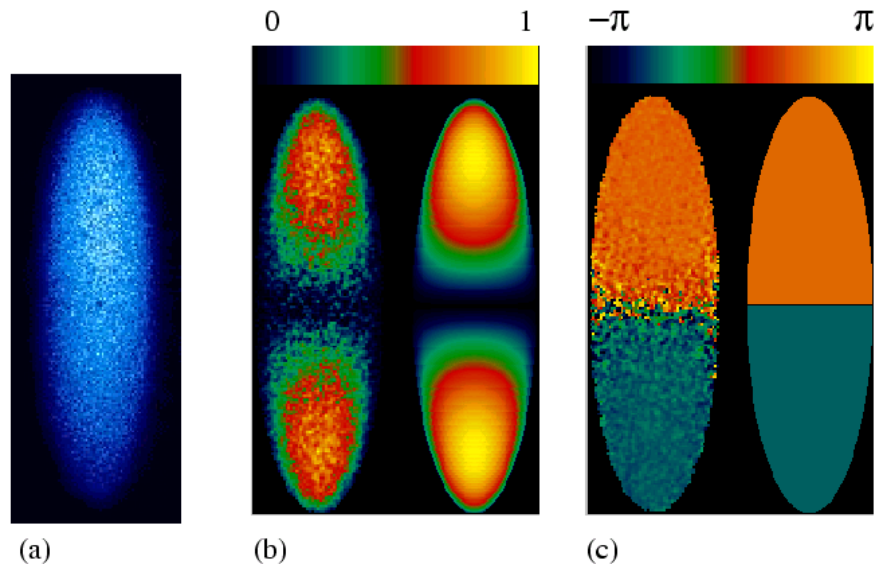
Figure 3.   (a) Movie of sideview image data obtained on a plasma with $\omega_r/2\pi=$ 1.00 MHz while driving a (2,0) mode at $\omega_{2,0}/2\pi=1.656$ MHz. The magnetic field and axial laser beam point up. The ion cloud dimensions are $2z_0 = 0.76$ mm and $2r_0 = 0.24$ mm, and the density $n_0 = 2.70 \times 10^9$ cm^{-3}. Comparison of the amplitude (b) and phase (c) extracted from the $(2,0)$ mode in (a) with the predictions of linear theory. The theory predictions are on the right.
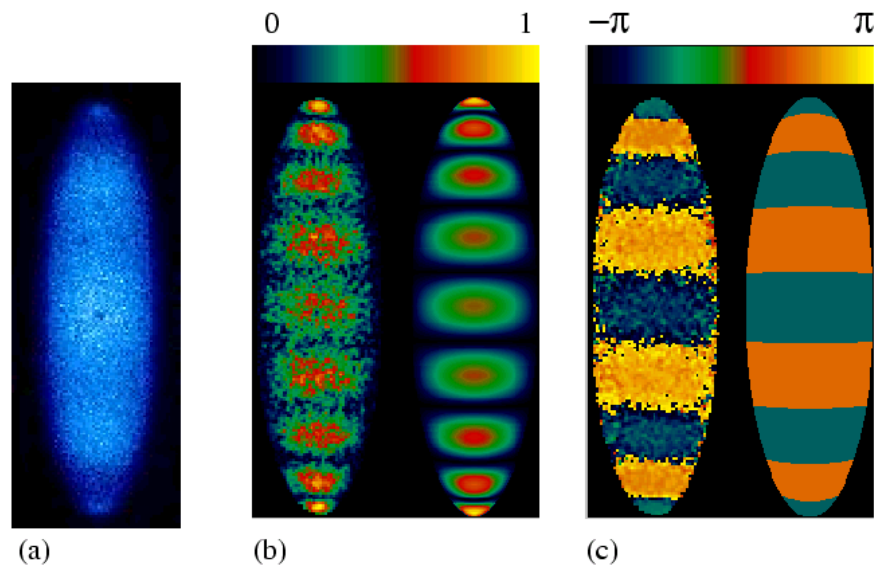

Figure 4.   (a) Movie of sideview image data obtained on the plasma of Fig. 3 with $\omega_r/2\pi=$ 1.00 MHz while driving a (9,0) mode at $\omega_{9,0}/2\pi=2.952$ MHz. Comparison of the amplitude (b) and phase (c) extracted from the $(9,0)$ mode in (a) with the predictions of linear theory. The theory predictions are on the right.

experiment, and both amplitudes are normalized to one.

From the fitted values of $A_{2,0}$ and A_0 we can estimate the coherent ion mode velocities if the dependence of the ion fluorescence on velocity (through Doppler shifts)

is known. For the low temperatures of this experiment a good approximation is to assume a Lorentzian profile with a 19 MHz full-width-at-half-maximum due to the natural linewidth of the optical cooling transition. With the 20 MHz detuning used in this experiment, we estimate for the data of Fig. 3 that the maximum coherent mode velocity, which occurs at $z = \pm z_0$, is ~ 1.5 m/s. The spatial and density changes in the plasma spheroid for this excitation are too small to be resolved ($\Delta z/z_0, \Delta n/n_0 < 10^{-3}$). Therefore the observed variation in the fluorescence intensity is entirely due to Doppler shifts induced by the coherent ion velocities of the mode.
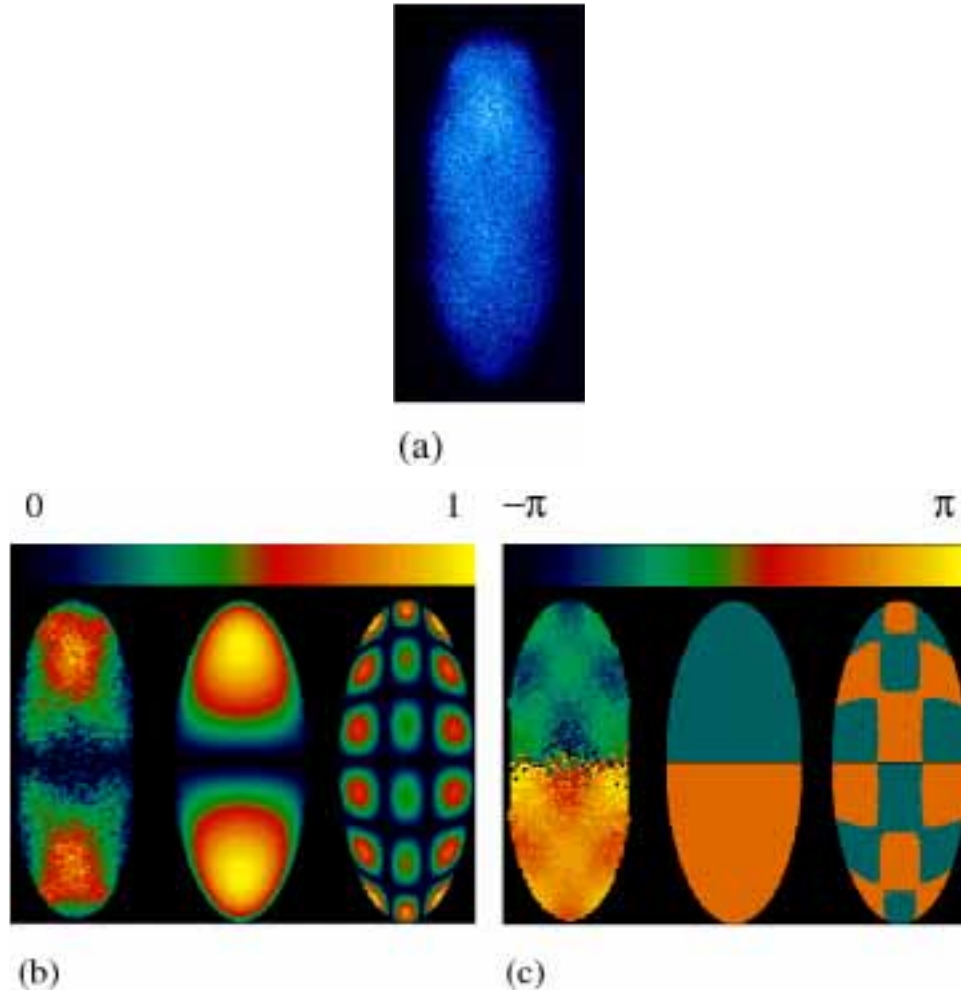

Figure 5.   (a) Movie of sideview image data obtained on a plasma with $\omega_r/2\pi =$ 638 kHz while driving with an even drive at 1.619 MHz. At this rotation frequency there is a crossing of the $(2, 0)$ mode and an $(8, 0)$ mode with a radial node. Comparison of the amplitude (b) and phase (c) extracted from the data in (a) with the predictions of linear theory. The predictions of both the $(2, 0)$ and $(8, 0)$ modes are given. For this plasma $2z_0 = 0.70$ mm and $2r_0 = 0.29$ mm.

We have measured the mode eigenfunctions of a number of different azimuthally symmetric ($m=0$) modes including the $l=2,3,4,5,7$ and 9 modes. Like the data of Fig. 3, good agreement with the predicted eigenfunction amplitude and phase distribution is obtained in the limit of low laser power and drive amplitude. Surprisingly high-order odd modes could be excited with the odd drive on the trap endcaps. Figure 4(a)

shows a sequence of 18 sideview images obtained with the $(9,0)$ excited by a drive at $\omega_{9,0}/2\pi = 2.952$ MHz. Figures 4(b) and 4(c) show the fitted amplitude and phase from this sequence, along with the predictions from theory. Similar high-order even $(l,0)$ modes are more difficult to excite.

Finally, Fig. 5 shows images from a plasma with $\omega_r/2\pi = 638$ kHz driven by an even drive at 1.619 MHz. This case demonstrates the utility of the Doppler imaging diagnostic. These data were initially taken during a survey of the $(2,0)$ mode eigenfunction as a function of the plasma's rotation frequency. Analysis of the phase-coherent data revealed additional, higher-order structure. An examination of the predictions for the mode frequencies revealed that at this particular rotation frequency, as shown in Fig. 2, both the $(2,0)$ mode and an $(8,0)$ mode with a radial node have similar frequencies. Characteristics of both modes are seen in the data. Measurements of the $(2,0)$ mode frequency near this crossing indicate that any frequency shifts due to a non-linear coupling with the $(8,0)$ mode are less than a few kilohertz. We note that the $(2,0)$ mode driven in Fig. 3 occurs near a crossing with a $(9,0)$ mode (see Fig. 2). In this case, no evidence for the excitation of a $(9,0)$ is observed, presumably because this is an odd mode.

5. Summary and conclusion

We have described a technique for imaging the eigenfunctions of a laser-cooled ion plasma. In general, for the azimuthally symmetric modes on spheroidal plasmas discussed here, good agreement is obtained between linear theory and experimental measurements made with low mode drive amplitude and laser power. The technique should be a useful tool for studying deviations from the linear theory, such as large amplitude frequency shifts and non-linear corrections to the mode eigenfunction. Data like that of Fig. 5 should be useful for studying the coupling between modes. Finally, the width of the resonant lineshape of the mode amplitude as a function of the drive frequency provides a measurement of the mode damping. With low laser power and a sufficiently clean plasma this should provide information on the viscosity of a strongly correlated plasma.

6. Acknowledgments